

CRASH: Raw Audio Score-based Generative Modeling for Controllable High-resolution Drum Sound Synthesis

Simon Rouard*
Sony CSL - CentraleSupélec
simon.rouard@student-cs.fr

Gaëtan Hadjeres*
Sony CSL
gaetan.hadjeres@sony.com

Abstract

In this paper, we propose a novel score-base generative model for unconditional raw audio synthesis. Our proposal builds upon the latest developments on diffusion process modeling with stochastic differential equations, which already demonstrated promising results on image generation. We motivate novel heuristics for the choice of the diffusion processes better suited for audio generation, and consider the use of a conditional U-Net to approximate the score function. While previous approaches on diffusion models on audio were mainly designed as speech vocoders in medium resolution, our method termed CRASH (Controllable Raw Audio Synthesis with High-resolution) allows us to generate short percussive sounds in 44.1kHz in a controllable way. Through extensive experiments, we showcase on a drum sound generation task the numerous sampling schemes offered by our method (unconditional generation, deterministic generation, inpainting, interpolation, variations, class-conditional sampling) and propose the class-mixing sampling, a novel way to generate “hybrid” sounds. Our proposed method closes the gap with GAN-based methods on raw audio, while offering more flexible generation capabilities with lighter and easier-to-train models.

1. Introduction and Related Work

After multiple works in the spectral domain Vasquez and Lewis [2019], Engel et al. [2019], deep generative models in the waveform domain have recently shown the ability to produce high fidelity results with different methods: autoregressive van den Oord et al. [2016], Mehri et al. [2017], flow-based Prenger et al. [2018], energy-based Gritsenko et al. [2020] or based on Generative Adversarial Networks Donahue et al. [2019].

In the task of generating drum sounds in the waveform domain, GAN-based approaches have been explored in Don-

ahue et al. [2019] and Nistal et al. [2020]. However, the authors can generate only low-resolution 16kHz drum sounds which is often unacceptable for music producers. Interactive sound design is often a major motivation behind these works: in Aouameur et al. [2019] the authors use Variational Autoencoders (VAE) in order to generate spectrograms of drums apply a principal component analysis on the latent space of the VAE in order to explore the drum timbre space. One of the disadvantages of this model is that the reconstruction of the sounds by the VAE tends to be blurry. In Bazin et al. [2021], the authors use a VQ-VAE2 Razavi et al. [2019] in order to perform inpainting on instrument sound spectrograms.

Score-based generative models Vincent [2011], Ho et al. [2020], Song and Ermon [2019], Song et al. [2021a] propose a different approach to generative modeling, which consists in estimating the gradient of noise-corrupted data log-densities (score function): by iteratively denoising a sampled noise, these approaches obtained promising results, but mainly on image data. Moreover, the authors of Denoising Diffusion Implicit Model (DDIM) Song et al. [2021b] use non-Markovian diffusion processes in order to accelerate the sampling of diffusion models.

To this day, only two score-based generative models in the waveform domain have been published Kong et al. [2021], Chen et al. [2020] and they are mostly focused on the task of neural vocoding with conditioning on a mel-spectrogram. In Kong et al. [2021], the authors achieved the task of generating audio with an unconditioned model trained on the speech command dataset Warden [2018]. The inference scheme of Kong et al. [2021] does not provide a flexible sampling scheme because it is trained on a fixed discrete noise schedule whereas Chen et al. [2020] is trained on a continuous scalar indicating the noise level.

In the image domain, Song et al. [2021a] generalizes the works of Sohl-Dickstein et al. [2015], Ho et al. [2020], Song and Ermon [2019] by framing the noise corruption procedure as stochastic differential equation.

Score-based generative models offer the following advantages over GAN-based approaches:

*Equal contribution

- Training time is reduced and training is more stable since there is only one network to train.
- Class-conditioning generation can be achieved by training a classifier a posteriori, which lets us train a model only one time.
- Data can be mapped to a latent space without the need to train an additional encoder compared to GANs Tov et al. [2021], which makes the interpolation between two given input data readily available with only one model.

These properties alleviate us to search for directions in the latent space as in Härkönen et al. [2020] or to directly hard-code conditional features in the architecture as in Mirza and Osindero [2014]. This easily controllable latent space permits sound design applications. One downside of score-based models compared to GANs is their higher inference times to generate new samples.

In this work, we extend the approach of Song et al. [2021a] and propose CRASH (Controllable Raw Audio Synthesis with High-resolution), a score-based generative model adapted to the waveform domain. On a drum sound dataset, the numerous capabilities offered by this architecture allows for musically-relevant sound design applications. Our contributions are the following:

- A score-based model for unconditional generation that can achieve high fidelity 44.1 kHz drum sounds directly in the waveform domain,
- The use of a noise-conditioned U-Net to estimate the score function,
- A novel *class-mixing* sampling scheme to generate "hybrid" sounds.
- We provide a reparameterization of the SDE that shows that the DDIM deterministic sampling is another discretization of Song et al. [2021a] which leads to faster than real time sampling.
- Experimental and practical insights about the choice of the stochastic differential equation used to corrupt the data.

2. Background

2.1. Score Based Modelling through Stochastic Differential Equations

2.1.1 Forward Process

Let p_{data} be a data distribution. Diffusion models consist in progressively adding noise to the data distribution to transform it into a known distribution from which we can sample from as shown in Fig. 1. In Song et al. [2021a], the authors

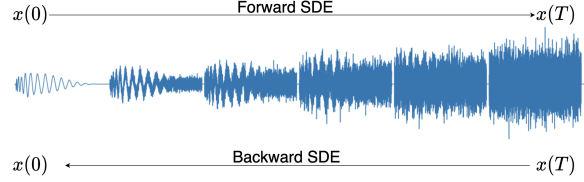


Figure 1. Illustration of the noising and denoising processes of a kick sound with a VP schedule

formalize this noising process as the following **forward** Stochastic Differential Equation (SDE):

$$dx = f(t)x dt + g(t) dw \quad (1)$$

where $f(t)$ is a continuous negative function from $[0, T] \rightarrow \mathbb{R}^-$, $g(t)$ a continuous positive function from $[0, T] \rightarrow \mathbb{R}^+$, and w is a standard Wiener process. Such approach can be understood as a continuous-time generalization of Denoising Diffusion Probabilistic Models (DDPMs) Sohl-Dickstein et al. [2015], Ho et al. [2020] and denoising Score Matching with Langevin Dynamics (SMLD) Song and Ermon [2019]. For $x(0) \sim p_{\text{data}}$, the transition kernel of Eq. 1 is given by a normal distribution:

$$p_t(x(t) | x(0)) = \mathcal{N}(x(t); m(t)x(0), \sigma^2(t)\mathbf{I}), \quad (2)$$

where $m(t)$ and $\sigma(t)$ follow the system:

$$\begin{cases} \frac{dm}{dt} = f(t)m(t) \\ \frac{d\sigma^2(t)}{dt} = 2f(t)\sigma^2(t) + g^2(t) \end{cases} \quad (3)$$

with the following initial conditions $m(0) = 1$ and $\sigma^2(0) = 0$.

The solutions for $m(t)$ and $\sigma(t)$ are :

$$\begin{cases} m(t) = e^{\int_0^t f(s)ds} \\ \sigma^2(t) = e^{\int_0^t 2f(s)ds} \int_0^t g^2(u) e^{\int_0^u -2f(s)ds} du. \end{cases} \quad (4)$$

In Song et al. [2021a], the authors define three types of SDEs which are presented in Tab. 1.

	$f(t)$	$g(t)$
VP	$-\frac{1}{2}\beta(t)$	$\sqrt{\beta(t)}$
VE	0	$\sqrt{\frac{d[\sigma^2(t)]}{dt}}$
sub-VP	$-\frac{1}{2}\beta(t)$	$\sqrt{\beta(t)(1 - e^{-2\int_0^t \beta(s)ds})}$

Table 1. Functions used in the VP, VE and sub-VP SDEs

For the Variance Preserving (VP) and sub-Variance Preserving (sub-VP) schedules, $m(T) \approx 0$ and $\sigma(T) \approx 1$ which means that the original data distribution is transformed into a distribution close to a standard normal distribution i.e. $p_T \approx \mathcal{N}(\mathbf{0}, \mathbf{I})$. For the Variance Exploding (VE), $\sigma^2(T) \gg m \approx 1$ which means that the original data is not perceptible at $t = T$ and that $p_T \approx \mathcal{N}(\mathbf{0}, \sigma^2(T)\mathbf{I})$.

2.1.2 Generation with the Reverse Process

In order to sample from the data distribution, we can sample $\mathbf{x}_T \sim p_T$ and apply the associated reverse time SDE Anderson [1982] given by:

$$d\mathbf{x} = [f(t)\mathbf{x} - g^2(t)\nabla_{\mathbf{x}} \log p_t(\mathbf{x})] dt + g(t) d\tilde{\mathbf{w}} \quad (5)$$

where $\tilde{\mathbf{w}}$ is a standard Wiener process running backwards from T to 0 and dt is an infinitesimal negative timestep.

It means that by knowing $\nabla_{\mathbf{x}} \log p_t(\mathbf{x})$, we can use a discretization of Eq. 5 to sample $\mathbf{x}(0)$ from $p_0 = p_{\text{data}}$.

In practice, the score function $s(\mathbf{x}(t), \sigma(t)) = \nabla_{\mathbf{x}} \log p_t(\mathbf{x})$ is intractable and it is approximated by a neural network $s_{\theta}(\mathbf{x}(t), \sigma(t))$ parameterized by θ . In order to train the network, Vincent [2011] shows that for any t , minimizing

$$\mathbb{E}_{p_t(\mathbf{x})} \|s_{\theta}(\mathbf{x}, \sigma(t)) - \nabla_{\mathbf{x}} \log p_t(\mathbf{x})\|_2^2 \quad (6)$$

is equivalent to minimizing

$$\mathbb{E} \|s_{\theta}(\mathbf{x}, \sigma(t)) - \nabla_{\mathbf{x}} \log p_t(\mathbf{x}(t) | \mathbf{x}(0))\|_2^2 \quad (7)$$

where the expectation is over $\mathbf{x}(0) \sim p_{\text{data}}$, $\mathbf{x}(t) \sim p_t(\mathbf{x}(t) | \mathbf{x}(0))$, and the latter distribution is given by Eq. 2.

Now, in order to train the network for all $t \in [0, T]$ we consider the following mixture of Eq. 7 losses over all noise levels:

$$L(\theta) = \mathbb{E} \lambda(t) \|s_{\theta}(\mathbf{x}(t), \sigma(t)) - \nabla_{\mathbf{x}(t)} \log p_t(\mathbf{x}(t) | \mathbf{x}(0))\|_2^2 \quad (8)$$

where we sample $t \sim [0, T]$, $\mathbf{x}(0) \sim p_{\text{data}}$, $\mathbf{x}(t) \sim p_t(\mathbf{x}(t) | \mathbf{x}(0))$ and where $\lambda(t)$ is a weighting function.

In Ho et al. [2020], Song and Ermon [2019], Song et al. [2021a], $\lambda(t)$ is empirically set such that $\lambda(t)^{-1} \propto \mathbb{E} \|\nabla_{\mathbf{x}(t)} \log p_t(\mathbf{x}(t) | \mathbf{x}(0))\|_2^2 \propto \sigma^2(t)^{-1}$ while in Durkan and Song [2021] the authors show that the maximum likelihood estimator is obtained with $\lambda(t) = g^2(t)$ in $L(\theta)$.

The training procedure is described in Alg. 1, where we reparameterize our neural network as $\epsilon_{\theta}(\mathbf{x}(t), \sigma(t)) := -\sigma(t)s_{\theta}(\mathbf{x}(t), \sigma(t))$ in order to estimate ϵ .

Algorithm 1 Training procedure

```

while Training do
  Sample  $t \sim \mathcal{U}([0, T])$ ,  $\mathbf{x}(0) \sim p_{\text{data}}$ ,  $\epsilon \sim \mathcal{N}(\mathbf{0}, \mathbf{I})$ 
  Compute  $\mathbf{x}(t) = m(t)\mathbf{x}(0) + \sigma(t)\epsilon$ 

  Gradient descent on  $\nabla_{\theta} \left\| \frac{\sqrt{\lambda(t)}}{\sigma(t)} [\epsilon_{\theta}(\mathbf{x}(t), \sigma(t)) - \epsilon] \right\|_2^2$ 
end while

```

Once the network is trained, a N-step discretization of the **reverse time** SDE is done in order to unconditionally generate samples. This process is described in Alg. 2, it is non-deterministic since we obtain various sounds by starting from the same sample $\mathbf{x}(T)$.

Algorithm 2 Sampling via SDE

```

Choose  $N$ , sample  $\mathbf{x}_N \sim \mathcal{N}(\mathbf{0}, \sigma^2(T)\mathbf{I})$ 
for  $i = N - 1, \dots, 0$  do
   $t_i = T \frac{i}{N}$ ,  $f_i = f(t_i)$ ,  $g_i = g(t_i)$ ,  $\sigma_i = \sigma(t_i)$ 
   $\mathbf{x}_i = (1 - \frac{f_{i+1}}{N})\mathbf{x}_{i+1} - \frac{g_{i+1}^2}{N\sigma_{i+1}}\epsilon_{\theta}(\mathbf{x}_{i+1}, \sigma_{i+1})$ 
  if  $i > 0$  then
    Sample  $\mathbf{z}_{i+1} \sim \mathcal{N}(\mathbf{0}, \mathbf{I})$ 
     $\mathbf{x}_i = \mathbf{x}_i + \frac{g_{i+1}}{\sqrt{N}}\mathbf{z}_{i+1}$ 
  end if
end for

```

2.2. Deterministic Sampling via Score based Ordinary Differential Equation

As mentioned in Song et al. [2021a], for any SDE, there exists a corresponding deterministic process which satisfies an ordinary differential equation (ODE):

$$d\mathbf{x} = [f(t)\mathbf{x} - \frac{1}{2}g^2(t)\nabla_{\mathbf{x}} \log p_t(\mathbf{x})] dt \quad (9)$$

This defines a flow ϕ^t such that the marginal distributions $\phi_*^t(p_{\text{data}})$ are identical to the ones obtained by applying the SDE of Eq. 1. This mapping is interesting because it provides a latent representation for each $\mathbf{x} \sim p_{\text{data}}$.

The procedure of sampling via the N-step discretization of the ODE is described in Alg. 3. Moreover, we also experimented sampling by using the `scipy.integrate.solve_ivp` solver with the RK45 method.

Algorithm 3 Sampling via ODE

```

Choose  $N$ , sample  $\mathbf{x}_N \sim \mathcal{N}(\mathbf{0}, \sigma^2(T)\mathbf{I})$ 
for  $i = N - 1, \dots, 0$  do
   $t_i = T \frac{i}{N}$ ,  $f_i = f(t_i)$ ,  $g_i = g(t_i)$ ,  $\sigma_i = \sigma(t_i)$ 
   $\mathbf{x}_i = (1 - \frac{f_{i+1}}{N})\mathbf{x}_{i+1} - \frac{g_{i+1}^2}{2N\sigma_{i+1}}\epsilon_{\theta}(\mathbf{x}_{i+1}, \sigma_{i+1})$ 
end for

```

2.3. Inpainting

Let's imagine that we don't like the attack of a kick (or any other part of a sound), the method of inpainting permits us to regenerate the desired part. In order to do that, we apply a reverse-time SDE or ODE discretization to an isotropic Gaussian and fix the part that we want to keep (with the associated noise corruption) after each denoising timestep. As presented in section 7, we obtain very diverse and coherent results.

Algorithm 4 Inpainting via ODE or SDE

Choose N, U an inpainting mask, $\mathbf{x}_{\text{fixed}}$ a fixed sound, sample $\mathbf{x}_N \sim \mathcal{N}(\mathbf{0}, \sigma^2(T)\mathbf{I})$

for $i = N - 1, \dots, 0$ **do**

$t_i = T \frac{i}{N}, f_i = f(t_i), g_i = g(t_i), \sigma_i = \sigma(t_i), m_i = m(t_i)$

if ODE Sampling **then**

$\mathbf{x}_i = (1 - \frac{f_{i+1}}{N})\mathbf{x}_{i+1} - \frac{g_{i+1}^2}{2N\sigma_{i+1}}\epsilon_\theta(\mathbf{x}_{i+1}, \sigma_{i+1})$

end if

if SDE Sampling **then**

$\mathbf{x}_i = (1 - \frac{f_{i+1}}{N})\mathbf{x}_{i+1} - \frac{g_{i+1}^2}{N\sigma_{i+1}}\epsilon_\theta(\mathbf{x}_{i+1}, \sigma_{i+1})$

if $i > 0$ **then**

Sample $\mathbf{z}_{i+1} \sim \mathcal{N}(\mathbf{0}, \mathbf{I})$

$\mathbf{x}_i = \mathbf{x}_i + \frac{g_{i+1}}{\sqrt{N}}\mathbf{z}_{i+1}$

end if

end if

Sample $\mathbf{z} \sim \mathcal{N}(\mathbf{0}, \mathbf{I})$

$\mathbf{x}_i \odot U = m_i(\mathbf{x}_{\text{fixed}} \odot U) + \sigma_i(\mathbf{z} \odot U)$

end for

2.4. Interpolations

The flexibility of SDEs and ODEs allows to compute interpolations between sounds. In fact, there exists an infinity of latent spaces indexed by $t \in [0, T]$. We present here two types of interpolations: ODE interpolation in the latent space of isotropic Gaussians and SDE interpolation in any t-indexed latent space.

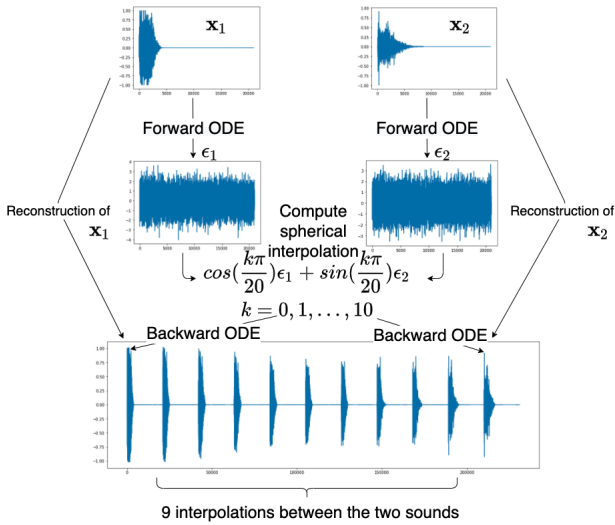


Figure 2. Interpolation of two sounds via Forward and Backward ODE

2.4.1 ODE interpolation in the latent space of isotropic Gaussians

Let ϵ_1 and ϵ_2 be two samples from a standard normal distribution of \mathbb{R}^L where L is our space dimension and $0 \leq \lambda \leq 1$. We consider the spherical interpolation $\epsilon_\lambda = \lambda\epsilon_1 + \sqrt{1 - \lambda^2}\epsilon_2$ and then apply the ODE sampling to it. We choose a spherical interpolation in order to preserve a variance close to 1 for ϵ_λ .

Moreover, if we want to interpolate two sounds \mathbf{x}_1 and \mathbf{x}_2 , we can apply the Forward ODE in order to obtain the corresponding latent codes ϵ_1 and ϵ_2 , apply the desired spherical interpolation and then apply an ODE sampling.

2.4.2 ODE interpolation in a t-indexed latent space

In Kong et al. [2021], the authors perform a linear interpolation between two sounds at a corresponding intermediate t-indexed latent space before applying Denoising Diffusion Probabilistic Model (DDPM is the discrete equivalent of a VP SDE). We adapt the method to the continuous framework with SDE and ODE. Here again, the interpolation can be done between two t-indexed latent codes or between sounds corrupted using the transition kernel of Eq. 2.

2.5. Class-Conditional sampling with a classifier

For any class y , we can train a noise-conditioned classifier on corrupted data $\mathbf{x}(t)$. As a consequence, the output of the classifier gives us $p_t(y | \mathbf{x}(t))$ for each class y . We can use automatic-differentiation to differentiate this quantity and by the Bayes Formula, since $p(y)$ is constant for each class y , we have the following formula:

$$\nabla_{\mathbf{x}} \log p_t(\mathbf{x} | y) = \nabla_{\mathbf{x}} \log p_t(\mathbf{x}) + \nabla_{\mathbf{x}} \log p_t(y | \mathbf{x}) \quad (10)$$

As a consequence, we can generate samples of one class by solving this reverse time SDE:

$$d\mathbf{x} = [f(t)\mathbf{x} - g^2(t)\nabla_{\mathbf{x}} \log p_t(\mathbf{x} | y)] dt + g(t) d\tilde{\mathbf{w}} \quad (11)$$

This approach is flexible since it only requires to train a noise-conditioned classifier: there is no need to design and train a class-conditional score-based model as done in Kong et al. [2021].

3. Reparameterizing the SDE and ODE and link between ODE and DDIM

As shown in Sect. A, for any SDE we can reparameterize it by using the associated perturbation kernel and obtain the following forward SDE for $\frac{\mathbf{x}}{m}$:

$$d\left(\frac{\mathbf{x}}{m}\right) = \sqrt{\frac{d}{dt}\left(\frac{\sigma^2}{m^2}\right)} d\mathbf{w}. \quad (12)$$

According to Eq. 5, the associated reverse time SDE is (see Sect. A for details):

$$d\left(\frac{\mathbf{x}}{m}\right) = 2\frac{d}{dt}\left(\frac{\sigma}{m}\right)\epsilon(\mathbf{x}, \sigma) dt + \sqrt{\frac{d}{dt}\left(\frac{\sigma^2}{m^2}\right)} d\tilde{\mathbf{w}} \quad (13)$$

where $\epsilon(\mathbf{x}, \sigma) := -\sigma(t)\nabla_{\mathbf{x}} \log p_t(\mathbf{x})$.

In the same way, if we compute the associated deterministic ODE, we obtain:

$$d\left(\frac{\mathbf{x}}{m}\right) = d\left(\frac{\sigma}{m}\right)\epsilon(\mathbf{x}, \sigma). \quad (14)$$

Moreover, this ODE is a refactored version of Eq. 9 divided by m . It means that Eq. 9 and Eq. 14 encode the same latent representation. Now, by integrating Eq. 14 between t_i and t_{i+1} (and by writing $\mathbf{x}_i := \mathbf{x}(t_i)$, $m_i := m(t_i)$, $\sigma_i := \sigma(t_i)$), we obtain:

$$\begin{aligned} \frac{\mathbf{x}_{i+1}}{m_{i+1}} - \frac{\mathbf{x}_i}{m_i} &= \int_{t_i}^{t_{i+1}} \frac{d}{dt} \left(\frac{\sigma(t)}{m(t)} \right) \epsilon(\mathbf{x}(t), \sigma(t)) dt \\ &\approx \int_{t_i}^{t_{i+1}} \frac{d}{dt} \left(\frac{\sigma(t)}{m(t)} \right) \epsilon(\mathbf{x}_{i+1}, \sigma_{i+1}) dt \quad (15) \\ &= \left(\frac{\sigma_{i+1}}{m_{i+1}} - \frac{\sigma_i}{m_i} \right) \epsilon(\mathbf{x}_{i+1}, \sigma_{i+1}) \end{aligned}$$

This discretization is exactly the deterministic one from Denoising Diffusion Implicit Models Song et al. [2021b] (DDIM). Empirically, Alg. 5 gives great samples with only 20 or 30 steps which permits to sample faster than real time. This comes from the fact that the only approximation error is due to $\epsilon(\mathbf{x}(t), \sigma(t)) \approx \epsilon(\mathbf{x}_{i+1}, \sigma_{i+1})$ between t_i and t_{i+1} .

Algorithm 5 DDIM sampling

Choose N , sample $\mathbf{x}_N \sim \mathcal{N}(\mathbf{0}, \sigma^2(T)\mathbf{I})$
for $i = N - 1, \dots, 0$ **do**
 $t_i = T \frac{i}{N}, m_i = m(t_i), \sigma_i = \sigma(t_i)$
 $\mathbf{x}_i = \frac{m_i}{m_{i+1}} \mathbf{x}_{i+1} + (\sigma_i - \sigma_{i+1} \frac{m_i}{m_{i+1}}) \epsilon_{\theta}(\mathbf{x}_{i+1}, \sigma_{i+1})$
end for

Algorithm 6 Reparameterized SDE Sampling

Choose N , sample $\mathbf{x}_N \sim \mathcal{N}(\mathbf{0}, \sigma^2(T)\mathbf{I})$
for $i = N - 1, \dots, 0$ **do**
 $t_i = T \frac{i}{N}, m_i = m(t_i), \sigma_i = \sigma(t_i)$
 $\mathbf{x}_i = \frac{m_i}{m_{i+1}} \mathbf{x}_{i+1} + 2(\sigma_i - \sigma_{i+1} \frac{m_i}{m_{i+1}}) \epsilon_{\theta}(\mathbf{x}_{i+1}, \sigma_{i+1})$
if $i > 0$ **then**
Sample $\mathbf{z}_{i+1} \sim \mathcal{N}(\mathbf{0}, \mathbf{I})$
 $\mathbf{x}_i = \mathbf{x}_i + \sqrt{\left(\frac{\sigma_{i+1} m_i}{m_{i+1}}\right)^2 - \sigma_i^2} \mathbf{z}_{i+1}$
end if
end for

4. A discussion about Choosing the Right SDE: a generalization of the sub-VP SDE

In this section $T = 1$.

4.1. The Signal to Noise Ratio (SNR)

As Eq. 12 shows, any SDE for \mathbf{x} is equivalent to a Variance Exploding SDE for $\frac{\mathbf{x}}{m}$. We define SNR as the *signal-to-noise ratio associated to the SDE* by $\text{SNR}(t) := \frac{m(t)^2}{\sigma(t)^2}$, as it completely determines the signal-to-noise ratio of $x(t)$ via $\text{SNR}(\mathbf{x}(t)) = \text{SNR}(t)\mathbb{E}[\mathbf{x}(0)^2]$. The quantities defined by the variations of $\text{SNR}(t)$ are more interpretable than the functions f and g when working with the SDE and ODE reparameterizations of Eq.12 and Eq.14. We test different functions in the experiments. Moreover, once that the SNR is defined, we still need to provide a function $m(t)$ (or equivalently $\sigma(t)$).

4.2. About the relation between $m(t)$ and $\sigma(t)$

The VP SDE is the continuous version of the Denoising Diffusion Probabilistic Model (DDPM) used in Ho et al. [2020] Kong et al. [2021] Chen et al. [2020]. One of the main features of this model is that the mean coefficient $m(t)$ of the perturbation kernel is linked to the standard deviation $\sigma(t)$ (or noise-level) by the following equation $m(t) = \sqrt{1 - \sigma^2(t)}$.

Moreover, without mentioning this fact, in Song et al. [2021a] the authors introduce the sub-VP SDE which is characterized by the following formula $m(t) = \sqrt{1 - \sigma(t)}$. They obtained their best results with this schedule. This formula leads to a SNR that decays faster and that has a higher limit value in $t = 1$. Since β is fixed, it also leads to a slowly increasing σ function near $t = 0$. (See Fig.3)

In this work, we explore four relations between m and σ described in Tab. 2 in order to study the influence of the decay of the SNR ratio. We also write the functions $f(t)$ and $g(t)$ for each of these 4 relations. For the rest of the paper we take the convention $f(t) := -\frac{1}{2}\beta(t)$ in order to compare the VP and sub-VP schedules with ours.

m - σ relation	$f(t)$	$g(t)$
$m = \sqrt{1 - \sigma^2}$ (VP)	$-\frac{1}{2}\beta(t)$	$\sqrt{\beta(t)}$
$m = \sqrt{1 - \sigma}$ (sub-VP)	$-\frac{1}{2}\beta(t)$	$\sqrt{\beta(t)(1 - e^{-2\int_0^t \beta(s)ds})}$
$m = 1 - \sigma$ (sub-VP 1-1)	$-\frac{1}{2}\beta(t)$	$\sqrt{\beta(t)(1 - e^{-\frac{1}{2}\int_0^t \beta(s)ds})}$
$m = (1 - \sigma)^2$ (sub-VP 1-2)	$-\frac{1}{2}\beta(t)$	$\sqrt{\beta(t)(1 - \frac{3}{2}e^{-\frac{1}{2}\int_0^t \beta(s)ds} + \frac{1}{2}e^{-\int_0^t \beta(s)ds})}$

Table 2. Functions used in the VP, sub-VP and generalized sub-VP SDEs. We give the general formulas in section D.

4.3. Choosing the right functions for the SDE

Choosing a particular relation between m and σ , imposes a relation between g and β . The remaining free parameter is

the function β , needed to fully define the SDE. In Song et al. [2021a], the authors use a linear schedule for $\beta(t)$ because it is the continuous generalization of DDPMs. As presented in Fig. 3, this choice leads to a $\sigma(t)$ function that rapidly grows to its maximum. In Nichol and Dhariwal [2021], the authors mention this fast growing σ function as a potential shortcoming and propose a smoother function (the green one in Fig. 3).

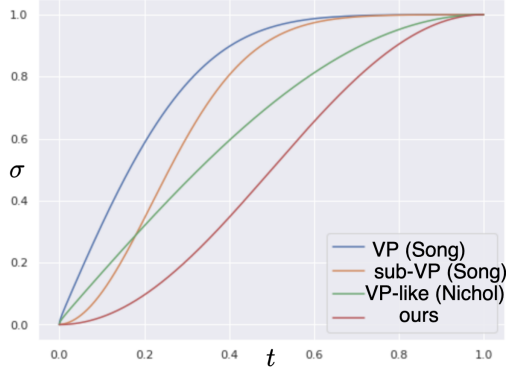


Figure 3. Different choices for the $\sigma(t)$ function

Our approach differs from Song et al. [2021a] in that the definition of our SDE is motivated by choosing a relatively smooth increasing function $\sigma(t)$ such as $\sigma(0) = 0$ and $\sigma(1) = 1 - \epsilon$ (where ϵ is a small constant), together with a m - σ relation, from which all other quantities can be computed as shown in Tab. 2. If the two approaches are equivalent, we believe that these quantities are more interpretable. In the regime of a small number of discretization steps, a slow increasing function may induce less approximation errors. For our experiments we propose $\sigma(t) = \frac{1}{2}[1 - \cos((1 - s)\pi t)]$ with $s = 0.006$ which is the red plot in Fig. 3. We also sample t in the interval $[\eta, 1]$ during the training where η is chosen such that $\sigma(\eta) = 10^{-4}$ because 10^{-4} is imperceptible.

5. Class-mixing sampling with a classifier

Drum classes are not perfectly distinct. For instance, the dataset contains drum sounds that are percussive enough to be seen as kicks but also sufficiently brilliant to be seen as snares and some kicks are combined with a hi-hat sound. We observe that our classifier (at the noise-level $\sigma = 0$) sometimes outputs a mixed classes such as $[0.3, 0.3, 0.4]$ and that it aligns well with our feeling when hearing the sound.

We introduce the Class-Conditional sampling to a mixture of classes: For a given noisy sound $\mathbf{x}(t)$, the vector $\nabla_{\mathbf{x}(t)} \log p_t(y_i | \mathbf{x}(t))$ points out to the direction of the class y_i in the noisy t -indexed latent space. Now, assuming that we have N classes $(y_i)_{i=1, \dots, N}$, let $(\lambda_i)_{i=1, \dots, N}$ be positive real numbers such as $\sum_{i=1}^N \lambda_i = 1$, we define a

mixture of classes that we note $\{(y_i, \lambda_i)\}$ and the associated vector:

$$\nabla_{\mathbf{x}} \log p_t(\{(y_i, \lambda_i)\} | \mathbf{x}) := \sum_{i=1}^N \lambda_i \nabla_{\mathbf{x}} \log p_t(y_i | \mathbf{x}) \quad (16)$$

In practice, we put this term in equation 10 in replacement of the last term and use equation 11 to sample class-mixed audios. It gives us interesting results with a great palette of sounds.

6. Architecture

6.1. Conditioned U-Net

Our model architecture is a conditioned U-Net Meseguer-Brocal and Peeters [2019], originally proposed for source separation. It takes two inputs: the noise level $\sigma(t)$ and the noisy audio $\mathbf{x}(t)$. The noise-level is encoded by Random Fourier Features Tancik et al. [2020] followed by a Multi-Layer Perceptron. The noisy audio goes into FiLM-conditioned Perez et al. [2017] Downsampling Blocks. Then, the signal goes into Upsampling Blocks that receive skip connections from the DBlocks of same levels. The output of the network is the estimated noise $\epsilon_{\text{estimated}}$.

This bears similarities with the architecture from Kong et al. [2021] which has a similar succession of blocks with dilated convolutions but no downsampling or upsampling layers, which makes it slow in terms of computation. The architecture from Chen et al. [2020] has a U-Net-like shape Ronneberger et al. [2015], but heavily depends on the spectrogram conditioning and relies on a different noise-conditioning scheme. The σ -conditioned U-Net architecture seems to retain advantages from both approaches and is particularly suited for unconditional generation (see Fig. 4). The details of the architecture are presented in Sect. C.

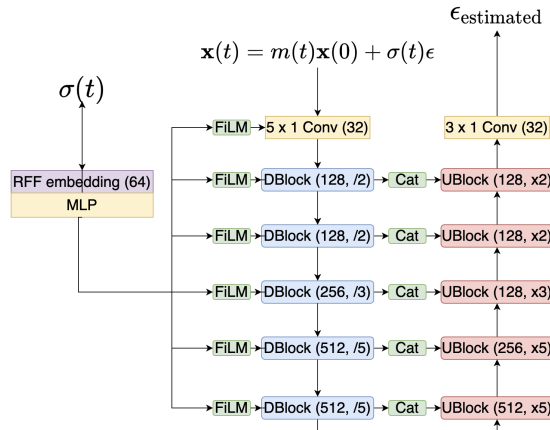


Figure 4. Architecture of the Conditioned U-Net

6.2. Noise conditioned classifier

Our noise-conditioned classifier closely mimics the architecture of our Conditioned U-Net presented in Sect. 6.1. The classifier is composed of a succession of FiLM-conditioned DBlocks followed by a projection layer and a softmax. Parameters for this architecture are presented in Sect. C.4.

7. Experiments and results

7.1. Dataset

For this work, we use an internal non-publicly available dataset of drum sounds which has also been used in Nistal et al. [2020]. It is composed of approximately 300.000 one-shot kick, snare and cymbal sounds in equal proportions. The samples have a sample rate of 44.1kHz and are recorded in mono. We restricted and padded the audio to 21.000 time-steps because most sounds last less than 0.5 second. We used 90% of the dataset in order to train our model.

7.2. Models and process

We evaluate the influence of $\sigma(t)$ and four m - σ schedules. The training of the network is done with a learning rate of 2.10^{-4} and the Adam optimizer. In parallel, smoothed weights with exponential moving average (EMA) with a rate of 0.999 are computed and saved at each step. For each model, the network is trained for about 120 epochs and the weights are saved each 8 epochs. We generated drum sounds with the regular weights and with the EMA weights and we observed the same phenomenon as in Song and Ermon [2020]: for the regular weights the quality of the sounds is not necessarily increasing with the training time whereas the EMA weights provide better and more homogeneous Fréchet Audio Distance Kilgour et al. [2019] (FAD) during training².

After generating 2700 sounds for each checkpoint of each model, we choose the best checkpoints and generate 27000 drum sounds for each. It takes 12 hours to generate 27000 drum sounds on a Nvidia RTX-3090 GPU with an ODE or SDE schedule of 400 steps and batches of 180 sounds per generation (maximum memory capacity). In comparison, it takes around 5 hours with the scipy solver and it takes only 1.5 hours a DDIM 50 steps discretization which is faster than real time (27000 drum sounds represents 3.5 hours of audio).

7.3. Quantitative Results

We report the FAD (lower is better) between the 27000 generated drum sounds and the test set for each unconditional generation with SDE and ODE (with a discretization

²We use the original implementation Kilgour et al. [2019] available at https://github.com/google-research/google-research/tree/master/frechet_audio_distance

of 400 steps), a DDIM discretization with 50 steps and the `scipy.integrate.solve_ivp` solver with `rtol = atol = 10-5`, `method='RK45'` parameters in Tab. 3. The cos schedule refers to the function $\sigma(t) = \frac{1}{2}[1 - \cos((1 - s)\pi t)]$ (the red one in Fig. 3) and the exp schedule corresponds to the function $\sigma(t) = \sqrt{1 - e^{-0.1t - 9.95t^2}}$ used in Song et al. [2021a] (the blue one in Fig. 3). Because adding Gaussian noise with a factor 10^{-4} is almost non perceptible, we also decided to compute the FAD between the generated samples and a noisy version of the test set where we corrupted the sounds with a 10^{-4} level of Gaussian noise. The DDIM sampling and Scipy solver generate samples that are a bit noisy at a non-perceptible level, this is why they perform better on the noisy test set. Moreover, note that the FAD between the test set and the noisy test set is 0.72 which means that the FAD is a very sensitive metric. As a consequence, by looking at Tab. 3 we can only say that the "cos schedule" is more adapted than the "exp schedule" from Song et al. [2021a] to audio data for equally spaced discretization steps because there are more steps near $\sigma = 0$ which is crucial in order to obtain non-noisy sounds. We cannot really say if some sub-VP schedules are better than others and we think that the comparison should be done on image data because the metrics are more meaningful that in the audio domain.

Finally, all models generate kicks, snares and cymbals in equal proportions but the generated samples are a bit less diverse than in the original dataset.

7.4. Interactive sound design

Audio samples for all experiments described in this section can be heard on the accompanying website: <https://crash-diffusion.github.io/crash/>.

7.4.1 Interpolations

The relative lack of diversity of the unconditional generation is not dramatic since the model can still perform interactive sound design by modifying existing samples from the dataset. In order to do that, we apply the forward ODE to an existing sound and obtain its corresponding noise in the latent space of isotropic Gaussians. As presented in Fig. 2, we can perform spherical combinations on the latent codes and apply the backward ODE to obtain interpolations. Moreover the reconstructed sounds (at the left and right of the schema) are accurate.

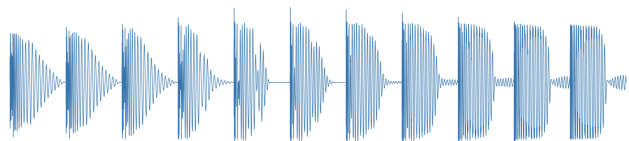


Figure 5. Interpolations between two kicks (at the left and right)

	Test Set				Noisy Test Set			
	SDE 400	ODE 400	Scipy	DDIM 50	SDE 400	ODE 400	Scipy	DDIM 50
VP exp schedule (as in Song et al. [2021a])	4.11	3.96	4.54	5.11	3.36	3.45	3.04	2.87
VP cos schedule	1.29	1.10	2.82	1.56	1.76	2.06	1.84	1.75
sub-VP cos schedule	1.34	0.98	3.08	3.36	1.71	1.56	1.81	1.49
sub-VP 1-1 cos schedule	1.41	1.23	2.92	2.93	1.67	2.45	2.11	1.53
sub-VP 1-2 cos schedule	1.69	1.51	1.66	5.24	2.22	2.85	1.43	3.96

Table 3. FAD comparison (lower is better)

7.4.2 Obtaining Variations of a Sound by Noising it and Denoising it via SDE

Let's take a sound $\mathbf{x}(0)$. We can noise it at a desired noise level $\sigma(t)$ via $\mathbf{x}(t) = m(t)\mathbf{x}(0) + \sigma(t)\epsilon$ and then denoise it with a SDE discretization from t to 0. We obtain then variations of the original sound.

7.4.3 Inpainting

We can also perform inpainting on a sound in order to regenerate any desired part. We show this method on Fig. 6 where we regenerate 6 endings of a snare sound.

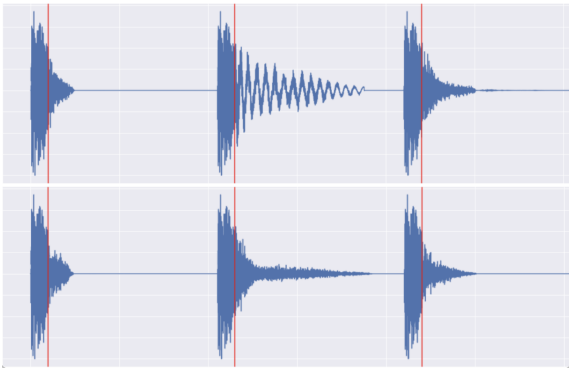


Figure 6. Six Inpaintings on the end of a snare sound

This provides an innovative way to generate a variety of plausible sounds starting with the same attack.

7.4.4 Class-Conditioning and Class-Mixing with a Classifier

We trained a noise-conditioned classifier on the 3 classes (kick, snare, cymbal) and used it to generate class-conditioned and class-mixing generation. Once again, by using the latent representation of a sound we can regenerate it (via ODE) with control on its "kickiness, snariness or cymbaliness".

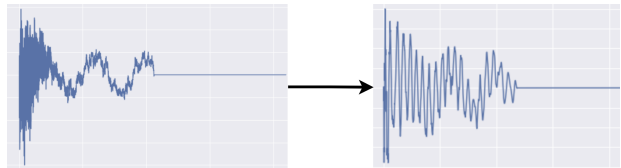


Figure 7. Transformation of a cymbal into a kick via class-conditioning ODE

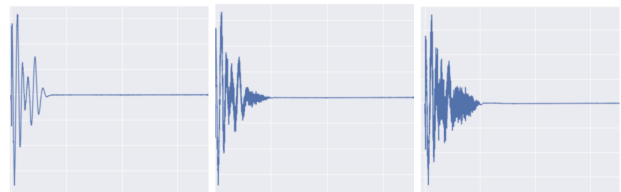


Figure 8. Modifying a kick to make it sounds more "snary" via class-mixing

8. Conclusion

We presented CRASH, a score-based generative model for the generation of raw audio based on the latest developments in modeling diffusion processes via SDEs. We proposed novel SDEs, well-suited to drum sound generation with high-resolution, together with an efficient architecture for estimating the score function. We showcased how the many controllable sampling schemes offered new perspectives for interactive sound design. In particular, our proposed *class-mixing* strategy allows the controllable creation of convincing "hybrid" sounds that would be hard to obtain with conventional means. We hope that these new methods will contribute to enrich the workflow of music producers.

References

- Sean Vasquez and Mike Lewis. Melnet: A generative model for audio in the frequency domain, 2019.
- Jesse Engel, Kumar Krishna Agrawal, Shuo Chen, Ishaan Gulrajani, Chris Donahue, and Adam Roberts. Gansynth: Adversarial neural audio synthesis, 2019.

- Aaron van den Oord, Sander Dieleman, Heiga Zen, Karen Simonyan, Oriol Vinyals, Alex Graves, Nal Kalchbrenner, Andrew Senior, and Koray Kavukcuoglu. Wavenet: A generative model for raw audio, 2016.
- Soroush Mehri, Kundan Kumar, Ishaan Gulrajani, Rithesh Kumar, Shubham Jain, Jose Sotelo, Aaron Courville, and Yoshua Bengio. Samplernn: An unconditional end-to-end neural audio generation model, 2017.
- Ryan Prenger, Rafael Valle, and Bryan Catanzaro. Waveglow: A flow-based generative network for speech synthesis, 2018.
- Alexey A. Gritsenko, Tim Salimans, Rianne van den Berg, Jasper Snoek, and Nal Kalchbrenner. A spectral energy distance for parallel speech synthesis, 2020.
- Chris Donahue, Julian McAuley, and Miller Puckette. Adversarial audio synthesis, 2019.
- J. Nistal, S. Lattner, and G. Richard. Drumgan: Synthesis of drum sounds with timbral feature conditioning using generative adversarial networks, 2020.
- Cyran Aouameur, Philippe Esling, and Gaëtan Hadjeres. Neural drum machine: An interactive system for real-time synthesis of drum sounds. In *International Conference on Computational Creativity*, 2019.
- Théis Bazin, Gaëtan Hadjeres, Philippe Esling, and Mikhail Malt. Spectrogram inpainting for interactive generation of instrument sounds. *arXiv preprint arXiv:2104.07519*, 2021.
- Ali Razavi, Aaron van den Oord, and Oriol Vinyals. Generating diverse high-fidelity images with vq-vae-2. *arXiv preprint arXiv:1906.00446*, 2019.
- Pascal Vincent. A connection between score matching and denoising autoencoders, 2011.
- Jonathan Ho, Ajay Jain, and Pieter Abbeel. Denoising diffusion probabilistic models, 2020.
- Yang Song and Stefano Ermon. Generative modeling by estimating gradients of the data distribution. In *Advances in Neural Information Processing Systems*, pages 11895–11907, 2019.
- Yang Song, Jascha Sohl-Dickstein, Diederik P. Kingma, Abhishek Kumar, Stefano Ermon, and Ben Poole. Score-based generative modeling through stochastic differential equations, 2021a.
- Jiaming Song, Chenlin Meng, and Stefano Ermon. Denoising diffusion implicit models. In *International Conference on Learning Representations*, 2021b. URL <https://openreview.net/forum?id=StlgIarCHLP>.
- Zhifeng Kong, Wei Ping, Jiayi Huang, Kexin Zhao, and Bryan Catanzaro. Diffwave: A versatile diffusion model for audio synthesis, 2021.
- Nanxin Chen, Yu Zhang, Heiga Zen, Ron J. Weiss, Mohammad Norouzi, and William Chan. Wavegrad: Estimating gradients for waveform generation, 2020.
- Pete Warden. Speech commands: A dataset for limited-vocabulary speech recognition, 2018.
- Jascha Sohl-Dickstein, Eric A. Weiss, Niru Maheswaranathan, and Surya Ganguli. Deep unsupervised learning using nonequilibrium thermodynamics, 2015.
- Omer Tov, Yuval Alaluf, Yotam Nitzan, Or Patashnik, and Daniel Cohen-Or. Designing an encoder for stylegan image manipulation. *CoRR*, abs/2102.02766, 2021. URL <https://arxiv.org/abs/2102.02766>.
- Erik Härkönen, Aaron Hertzmann, Jaakko Lehtinen, and Sylvain Paris. Ganspace: Discovering interpretable gan controls, 2020.
- Mehdi Mirza and Simon Osindero. Conditional generative adversarial nets, 2014.
- Brian D O Anderson. Reverse-time diffusion equation models, 1982.
- Conor Durkan and Yang Song. On maximum likelihood training of score-based generative models, 2021.
- Alex Nichol and Prafulla Dhariwal. Improved denoising diffusion probabilistic models, 2021.
- Gabriel Meseguer-Brocal and G. Peeters. Conditioned-u-net: Introducing a control mechanism in the u-net for multiple source separations. *ArXiv*, abs/1907.01277, 2019.
- Matthew Tancik, Pratul P. Srinivasan, Ben Mildenhall, Sara Fridovich-Keil, Nithin Raghavan, Utkarsh Singhal, Ravi Ramamoorthi, Jonathan T. Barron, and Ren Ng. Fourier features let networks learn high frequency functions in low dimensional domains, 2020.
- Ethan Perez, Florian Strub, Harm de Vries, Vincent Dumoulin, and Aaron Courville. Film: Visual reasoning with a general conditioning layer, 2017.
- Olaf Ronneberger, Philipp Fischer, and Thomas Brox. U-net: Convolutional networks for biomedical image segmentation, 2015.
- Yang Song and Stefano Ermon. Improved techniques for training score-based generative models, 2020.
- Kevin Kilgour, Mauricio Zuluaga, Dominik Roblek, and Matthew Sharifi. Fréchet audio distance: A metric for evaluating music enhancement algorithms, 2019.

A. Proof of the reparametrization

A.1. Forward SDE

By dividing Eq. 1 by m we have

$$\frac{d\mathbf{x}}{m(t)} = \frac{f(t)}{m(t)}\mathbf{x} dt + \frac{g(t)}{m(t)} d\mathbf{w}, \quad (17)$$

moreover, the first equation of Eq. 3 gives

$$f(t) dt = \frac{dm}{m(t)} \quad (18)$$

and Eq. 17 becomes

$$\frac{m(t) d\mathbf{x}}{m^2(t)} = \frac{\mathbf{x} dm}{m^2(t)} + \frac{g(t)}{m(t)} d\mathbf{w}. \quad (19)$$

By dividing the second relation of Eq. 3 by $m^2(t)$, we obtain the equation:

$$\frac{2\sigma(t)\sigma'(t)}{m^2(t)} = 2f(t)\frac{\sigma^2(t)}{m^2(t)} + \frac{g^2(t)}{m^2(t)}, \quad (20)$$

since $f(t) = \frac{m'(t)}{m(t)}$, we have then:

$$\frac{2\sigma(t)\sigma'(t)m^2(t) - 2m'(t)m(t)\sigma^2(t)}{m^4(t)} = \frac{g^2(t)}{m^2(t)}, \quad (21)$$

and since g and m are positive, this can be rewritten into:

$$\frac{g(t)}{m(t)} = \sqrt{\frac{d}{dt} \left(\frac{\sigma^2(t)}{m^2(t)} \right)}. \quad (22)$$

Equation 19 becomes then:

$$d \left(\frac{\mathbf{x}}{m} \right) = \sqrt{\frac{d}{dt} \left(\frac{\sigma^2}{m^2} \right)} d\mathbf{w}. \quad (23)$$

A.2. Reverse time SDE

According to Eq. 5, the associated reverse time SDE is:

$$d \left(\frac{\mathbf{x}}{m} \right) = -\frac{d}{dt} \left(\frac{\sigma^2}{m^2} \right) \nabla_{\frac{\mathbf{x}}{m}} \log q_t \left(\frac{\mathbf{x}}{m} \right) dt + \sqrt{\frac{d}{dt} \left(\frac{\sigma^2}{m^2} \right)} d\tilde{\mathbf{w}} \quad (24)$$

where $q_t \left(\frac{\mathbf{x}(t)}{m(t)} \mid \frac{\mathbf{x}(0)}{m(0)} \right) = \mathcal{N} \left(\frac{\mathbf{x}(t)}{m(t)}; \mathbf{x}(0), \frac{\sigma^2(t)}{m^2(t)} \mathbf{I} \right)$.

A quick calculus shows that:

$$\nabla_{\frac{\mathbf{x}}{m}} \log q_t \left(\frac{\mathbf{x}(t)}{m(t)} \mid \frac{\mathbf{x}(0)}{m(0)} \right) = m(t) \nabla_{\mathbf{x}} \log p_t(\mathbf{x}(t) \mid \mathbf{x}(0)). \quad (25)$$

Using the fact that $m(0) = 1$, by integrating over p_{data} we obtain:

$$\nabla_{\frac{\mathbf{x}}{m}} \log q_t \left(\frac{\mathbf{x}}{m} \right) = m(t) \nabla_{\mathbf{x}} \log p_t(\mathbf{x}(t)). \quad (26)$$

Then, by writing $\epsilon(\mathbf{x}, \sigma) := -\sigma(t) \nabla_{\mathbf{x}} \log p_t(\mathbf{x})$ we obtain:

$$\begin{aligned} -\frac{d}{dt} \left(\frac{\sigma^2}{m^2} \right) \nabla_{\frac{\mathbf{x}}{m}} \log q_t \left(\frac{\mathbf{x}}{m} \right) &= \frac{d}{dt} \left(\frac{\sigma^2}{m^2} \right) \frac{m}{\sigma} \epsilon(\mathbf{x}, \sigma) \\ &= 2 \frac{d}{dt} \left(\frac{\sigma}{m} \right) \epsilon(\mathbf{x}, \sigma) \end{aligned} \quad (27)$$

which gives us the reverse-time SDE:

$$d \left(\frac{\mathbf{x}}{m} \right) = 2 \frac{d}{dt} \left(\frac{\sigma}{m} \right) \epsilon(\mathbf{x}, \sigma) dt + \sqrt{\frac{d}{dt} \left(\frac{\sigma^2}{m^2} \right)} d\tilde{\mathbf{w}}. \quad (28)$$

A.3. Associated ODE

Finally, the associated ODE comes directly with a factor $\frac{1}{2}$ behind the drift of the reverse-time SDE:

$$d \left(\frac{\mathbf{x}}{m} \right) = \frac{d}{dt} \left(\frac{\sigma}{m} \right) \epsilon(\mathbf{x}, \sigma) dt. \quad (29)$$

B. About the link between an affine log SNR and the Maximum Likelihood Estimation

Let's consider a SNR such as $\log \text{SNR}(t)$ is affine. Then, we have $\frac{\sigma(t)^2}{m(t)^2} = e^{at+b}$. By using Eq. 22, we obtain $g(t)^2 = m(t)^2 a e^{at+b} = a m(t)^2 \frac{\sigma(t)^2}{m(t)^2} = a \sigma(t)^2$. This means that having an affine $\log \text{SNR}(t)$ is a situation where the maximum likelihood estimator is equivalent to the ancestral training method (where $\lambda(t) \propto \sigma(t)^2$).

C. Architectural details

C.1. Random Fourier Features Embeddings and FiLM

First, the embedding of σ is done with Random Fourier Features (RFF):

$$[\cos(2\pi f_1 \sigma), \dots, \cos(2\pi f_N \sigma), \sin(2\pi f_1 \sigma), \dots, \sin(2\pi f_N \sigma)] \quad (30)$$

with $N = 32$ and f_1, \dots, f_N are sampled from a one-dimensional Gaussian with zero mean and variance 16 and fixed for the whole training. Unlike other architectures, we make the choice of encoding σ instead of t because the network does not have to learn the function $\sigma(t)$. The RFF are followed by a MLP. For each DBlock, the embedding of σ is fed into a Linear layer of output size $2C_{\text{out}}$ that is chunked in order to obtain $\gamma(\sigma)$ and $\beta(\sigma)$ that are the factors of the FiLM-like operation.

C.2. Downsampling and Upsampling Blocks

The DBlocks begin with a Downsampling task: for instance if the downsampling factor is 3, only the first element of each sequence of 3 is kept. Then there is a first

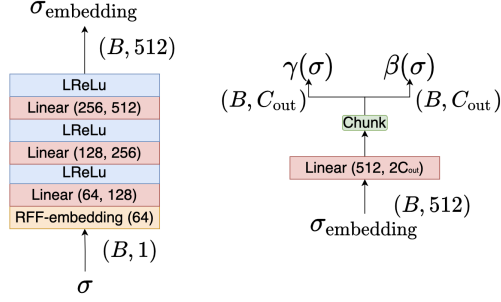


Figure 9. A Downsampling Block

1D-Convolution with an output channel size C_{out} equal to the output channel size of the Block. Then, a FiLM-like Perez et al. [2017] operation is done to the signal x of shape $(B, C_{\text{out}}, \frac{T}{f})$:

$$\gamma(\sigma) \odot x + \beta(\sigma) \quad (31)$$

After that, the signal goes into three 1-D convolutions. For the four 1-D convolutions of the main Block the dilation factors are 1, 2, 4, 8 and the kernel size is 3. For the residual Block the convolution has an output channel size C_{out} and a kernel size of 1.

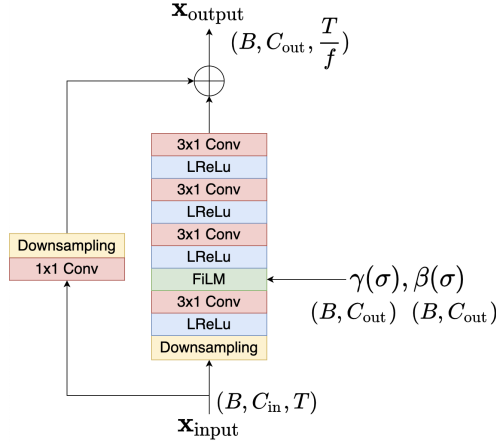


Figure 10. A Downsampling Block

The UBlocks are similar to the DBlocks but there are some little differences. The input $\mathbf{x}_{\text{input}}$ is concatenated with the output of the DBlock of the same level $\mathbf{x}_{\text{DBlock}}$. The concatenation which has the shape $(B, 2C_{\text{in}}, T)$ is upsampled (by repeating each number f time) and then goes into a 1-D convolution with dilation 1 number of output channels C_{out} . The following convolutions have dilation factors of 2, 4, 8.

C.3. About the U-Net

The downsampling and upsampling factors of our U-Net are 2, 2, 3, 5, 5 which means that the input audio must have a length divisible by 300. The number of channels of the outputs of the DBlocks are: 128, 128, 256, 512, 512.

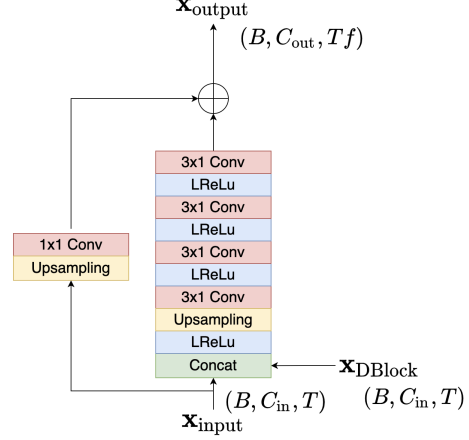


Figure 11. An Upsampling Block

C.4. About the noise-conditioned classifier

The noise-conditioned classifier is constituted of one 1D convolution with 32 channels with a kernel size of 5 and a padding of 2. Followed by 5 DBlocks with downsampling factors of 4, 3, 5, 25, 14 with outputs channels of size 128, 256, 512, 512, 512. There is a final linear layer of output size 3 followed by a softmax.

D. About the generalization of sub-VP

Considering the following forward SDE :

$$d\mathbf{x} = -\frac{1}{2}\beta(t)\mathbf{x} dt + g(t) d\mathbf{w} \quad (32)$$

The associated following system for m and σ is :

$$\begin{cases} \frac{dm}{dt} = -\frac{1}{2}\beta(t)m(t) \\ \frac{d\sigma^2(t)}{dt} = -\beta(t)\sigma^2(t) + g^2(t) \end{cases} \quad (33)$$

with the following conditions :

$$\begin{cases} m(0) = 1 \\ \sigma^2(0) = 0 \end{cases} \quad (34)$$

The solutions are :

$$\begin{cases} m(t) = e^{-\int_0^t \frac{1}{2}\beta(s)ds} \\ \sigma^2(t) = e^{-\int_0^t \beta(s)ds} \int_0^t g^2(u)e^{\int_0^u \beta(s)ds} du \end{cases} \quad (35)$$

Now, by applying the method described in 4, if we have chosen $\sigma(t)$ and a relation between m and σ in the form

$$m = (1 - \sigma^\gamma)^\eta \quad (36)$$

In order to calculate $\beta(t)$ and $g(t)$, the first equation of Eq. 33 gives the expression of β function of σ and its derivative σ' , the second equation gives $g(t)$:

$$\beta(t) = \frac{2\eta\gamma\sigma'(t)\sigma^{\gamma-1}(t)}{1 - \sigma^\gamma(t)} \quad (37)$$

$$g(t) = \sqrt{2\sigma'(t)\sigma(t)\left(\frac{\gamma\eta\sigma^\gamma(t)}{1-\sigma^\gamma(t)} + 1\right)} \quad (38)$$

and we can rewrite it as:

$$g(t) = (\beta(t))\left[\left(1 - e^{-\frac{1}{2\eta} \int_0^t \beta(s) ds}\right)^{\frac{2}{\gamma}} + \frac{1}{\gamma\eta} e^{-\frac{1}{2\eta} \int_0^t \beta(s) ds} \left(1 - e^{-\frac{1}{2\eta} \int_0^t \beta(s) ds}\right)^{\frac{2}{\gamma}-1}\right]^{\frac{1}{2}} \quad (39)$$